Proceedings of the 7th International Young Geotechnical Engineers Conference – Scott (Ed.)

Benchmark of small-strain shear modulus on Belgian North Sea soils with bender element testing

Analyse comparative du module de cisaillement à petite déformation sur les sols Belges de la mer du Nord avec essais des éléments piézoéléctriques

Diego Gómez & Bruno Stuyts
Geotechnics Laboratory/OWI-Lab, Ghent University, Belgium, diegoalexander.gomezbautista@ugent.be

ABSTRACT: Inaccurate foundation models for the design of offshore wind turbines (OWTs) monopiles have underestimated the small-strain soil stiffness and have resulted in a mismatch between the predicted and measured natural frequencies of the support structure. This foundation model flaw prevents the prediction of accurate fatigue loads and increases uncertainties in the estimated fatigue lifetime. In the framework of the SOILTWIN project of OWI-Lab, which aims to improve OWTs soil-structure interaction models by updating them based on advanced laboratory testing and in-situ monitoring data, this paper presents an experimental investigation to assess the shear modulus in the small-strain range for different Belgian North Sea soil units. Small-strain soil stiffness is assessed using a bender element setup incorporated on a stress path cell. The measurements are compared against in-situ measurements using the seismic piezocone (S-PCPT) and existing correlations with the piezocone (PCPT). These results will provide a new benchmark for past in-situ and laboratory stiffness measurements of soils in the region and allow for a proper modelling of small-strain behaviour to be included in the soil reaction curves employed in new design methodologies for offshore wind turbine monopiles.

RÉSUMÉ : Des modèles de fondation imprécis pour la conception des monopieux des éoliennes offshore (EO) ont sous-estimé la rigidité du sol à faible déformation et ont entraîné un décalage entre les fréquences naturelles prévues et mesurées de la structure de support. Ce défaut du modèle de fondation empêche la prédiction de charges de fatigue précises et augmente les incertitudes sur la durée de vie estimée en fatigue. Dans le cadre du projet SOILTWIN de OWI-Lab, qui vise à améliorer les modèles d'interaction sol-structure des EO en les mettant à jour sur la base d'essais avancés en laboratoire et de données de surveillance in-situ, cet article présente une enquête expérimentale pour évaluer le module de cisaillement dans le gamme de petites souches pour différentes unités de sol de la mer du Nord Belge. La rigidité du sol à petite déformation est évaluée à l'aide d'une configuration des éléments piézoéléctriques incorporée dans une cellule de chemin de contrainte. Les mesures sont comparées aux mesures in-situ utilisant le S-PCPT et les corrélations existantes avec le PCPT. Ces résultats fourniront une nouvelle référence pour les mesures antérieures de rigidité in situ et en laboratoire des sols de la région et permettront d'inclure une évaluation appropriée du comportement sous petite deformation du sol dans les courbes de réaction du sol utilisées dans les nouvelles méthodologies de conception des monopieux des éoliennes offshore.

KEYWORDS: bender elements; shear modulus; offshore wind turbine; monopile.

1 INTRODUCTION

Monopile foundations for offshore wind turbines remain the dominant foundation type worldwide for water depths below 40m. However, new design methodologies are pushing design boundaries to expand the application of large-diameter monopiles to deeper water (Byrne et al. 2017), potentially up to 60m deep. These new developments recognize the essential influence of the soil stiffness at small strains for the dynamic performance of the wind turbine system, assessed through the structural natural frequencies for design against fatigue damage. Therefore, a reliable assessment of the small-strain shear modulus (G_{max}) of the foundation soil is a vital priority for design and particularly for an accurate fatigue lifetime estimation of the monopile foundation (Aasen et al. 2017).

Elastic or maximum soil stiffness can be measured through different techniques which include seismic in-situ testing methods, such as seismic piezocone (S-PCPT) and non-invasive active methods (e.g. MASW, S-wave refraction/reflection); and advanced laboratory testing, such as resonant column and bender element testing (Jardine 2014). A laboratory programme was performed to assess the small-strain shear modulus for two Belgian North Sea soil units: Eemian sand and Wemmel sand. Small-strain soil stiffness is assessed using a bender element (BE) setup incorporated on a stress path cell. The measurements are compared against in-situ measurements using the S-PCPT and existing correlations with the PCPT. The work presented in this paper forms part of a research project on data-driven design optimization of monopile foundations using updated soil-structure interaction models. The general goal of the project is to calibrate these models by updating them based on finite element analysis, advanced laboratory testing and in-situ measurements coming from Belgian offshore wind farms. Advanced laboratory experiments are vital to accurately characterise the elasto-plastic strain-stress behaviour over a wide strain level range including dynamic, cyclic and static monotonic loading conditions. Therefore, following the methodology proposed by the PISA project (Byrne et al. 2017), these experimental results allow the calibration of a soil constitutive model to be employed in 3D finite element analyses for predicting the monopile lateral response and extracting non-linear soil-pile reaction curves, which is a key step to generate a fully coupled dynamic assessment of the entire offshore wind turbine system.

2 EXPERIMENTAL PROGRAMME

2.1 *Test materials*

Two sandy soil materials were tested for the current experimental investigation coming from sampled material at a Belgian offshore wind farm located approximately 46 km from the coast of Zeebrugge on the Bligh Bank. The first sand corresponds to a Quaternary deposit from the *Eemian* interglacial period, and the

second is a Palaeogene age sand from the *Wemmel* geological member. Eemian sand is a fine to medium-grained cohesionless quartzitic material with abundant shells, poorly graded and with medium dense to very dense in-situ relative density conditions. Wemmel sand is a grey glauconitic slightly to very clayey fine sand, gap-graded and with dense to very dense in-situ relative density. Table 1 presents the index properties of the soil materials tested in the laboratory. Figure 1 shows the particle size distribution curve for both sand materials obtained according to the standard practice for wet preparation of soil samples for sieving analysis. Maximum and minimum dry unit weights for the Eemian sand were determined according to the ASTM dry method (ASTM, 2006). Corresponding Wemmel sand values were adopted from past projects in the region and are identified with an asterisk in the following table.

Table 1. Index properties of the materials tested

Properties	*Eemian sand*	*Wemmel sand*
Uniformity coefficient, C_u	1.97	9.93
Specific gravity, G_s	2.63	2.68
Maximum void ratio, e_{max}	0.82	1.15*
Minimum void ratio, e_{min}	0.50	0.76*

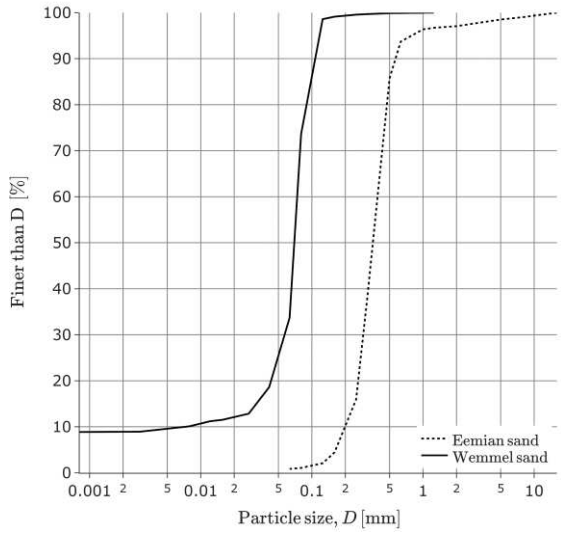

Figure 1. Particle size distributions of materials tested.

2.2 *Laboratory programme*

Thirteen bender element tests were performed in six different sand specimens at specific relative density conditions and effective consolidation stresses (σ'_c) simulating an in-situ stress state for each soil unit. All sand specimens were tested under isotropic effective stress conditions at UGent's geotechnics laboratory.

Eemian and Wemmel sand specimens were reconstituted with a target relative density varying from medium-dense to very dense conditions (D_r = 38 to 95%) as found from in-situ characterization performed in past local projects. Applied effective consolidation stresses were defined to simulate overburden pressures for soil depths between 8.5 to 35.0 m. All specimens were normally consolidated, excluding specimen TE-02, for which the impact of over-consolidation ratio (OCR = 1.48 to 2.45) was investigated. All tests were performed under saturated conditions, except for specimen TE-01, which due to technical issues was tested under partially saturated conditions. Table 2 presents an overview of the laboratory programme including the most important testing parameters and specimen ID.

Table 2. Summary of the testing programme

Specimen ID	*Material*	*Effective consolidation stress (kPa)*	*Relative density (%)*
TE-01	Eemian sand	85; 150	95
TE-02	Eemian sand	85; 170	45
TE-03	Eemian sand	85; 170	38
TE-04	Eemian sand	85; 105; 170	51
TW-01	Wemmel sand	135; 315	71
TW-02	Wemmel sand	135; 315	87

2.3 *Experimental set-up*

The apparatus used in this study was a stress path Bishop & Wesley triaxial testing system adapted with bender elements at the pedestal and top cap to measure the shear wave velocity propagating vertically through the sand sample. The bender element in the top cap is the transmitter which sends a horizontally polarised signal through the soil to the receiver bender element located in the pedestal. A digital oscilloscope with an integrated signal generator (Picoscope 2206) was used to create and monitor the electrical signals that were recorded as waveforms for further examination. The oscilloscope is also connected to an amplifier and a personal computer for data acquisition. Two digital pressure/volume controllers were used to apply consolidation and back-pressure in the sand specimens. Additionally, a de-aired water tank, a CO_2 gas cylinder and a vacuum/pressure system were utilized to reconstitute and saturate the soil specimens.

The bender element probes used in this experimental investigation were manufactured by GDS measuring 20 mm in length and 10 mm in width. The protrusion of the bender elements above the face of the pedestal and top cap was 8.66 mm and 2.57 mm, respectively. Figure 2 shows the bender element probes mounted into the triaxial apparatus.

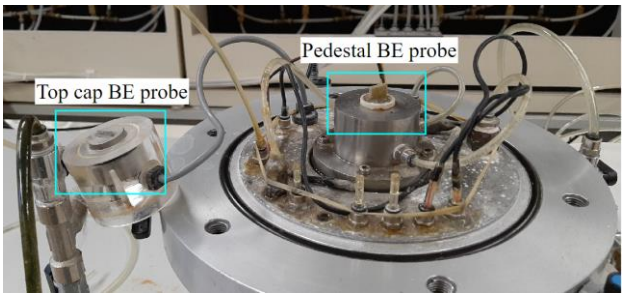

Figure 2. Bender elements probes into the triaxial pedestal and top cap.

2.4 *Specimen preparation procedure*

All sand specimens in this study were reconstituted according to the moist tamping technique and following the undercompaction method proposed by Ladd (1978) to achieve approximately uniform compaction throughout each specimen. Several studies have suggested that the moist tamping technique has a more consistent initial density control and better homogeneity compared with other sand specimen reconstitution techniques (e.g. Knudsen et al. 2019). Furthermore, this technique is commonly adopted at many geotechnical laboratories for industry projects.

A split compaction mold (D = 50 mm, H = 100 mm) attached to the triaxial pedestal was used to reconstitute the specimens

using a cylindrical tamper with a diameter of half the inner diameter of the mold. Nominal water content was adjusted to reach an initial degree of saturation of the compacted material between 20 to 70%, consequently, for Eemian specimens, it varied between 4 to 6%, while for Wemmel specimens it was raised to 15% due to an important increase in the percentage of fines. For medium-dense and dense specimens, the moist sand was tamped into the mold in six layers with an initial percent undercompaction factor of 2 and 1%, respectively, while for very dense specimens a factor of 0.3% was selected with ten layers for compaction. A vacuum of 0.8 bar was applied from a connection outside the split mold to tightly adjust the rubber membrane to the inner walls of the split mold. Figure 3 displays an example of a reconstituted sand specimen before triaxial cell assembly.

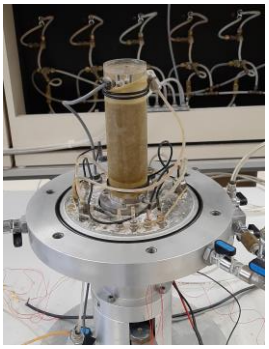

Figure 3. Reconstituted sand specimen by moist tamping technique.

2.5 *Test procedure*

After specimen preparation with the split mold, a vacuum of 20 kPa was applied to the specimen to increase effective stresses and sample stiffness during mold removal and triaxial cell assembly. Afterwards, an isotropic cell pressure of 20 kPa was applied while decreasing vacuum at the same rate. An efficient specimen saturation was reached by means of CO_2 and de-aired water percolation and flushing from bottom to top for 30 min and 1 h, respectively. Aiming to reach an adequate specimen saturation with a B-value of a minimum of 0.95, the back-pressure and cell pressure were increased simultaneously to pressures between 300 to 570 kPa always maintaining an effective consolidation stress equal to 20 kPa on the specimen. Back-pressure was held from 1 to 3 hours depending on the material to dissolve air bubbles in the water. Then, cell pressure was ramped up to isotropically consolidate the specimen to the corresponding effective consolidation stress as specified in Table 2. A resting period of approximately 1 to 2 h was considered for bender element tests in the same specimen at different consolidation stress levels, which was enough to reach primary consolidation for the tests herein. The repeatability of the bender element testing setup was verified by comparison of the tests results from three medium-dense Eemian sand specimens.

The optimal signal characteristics and interpretation method for the bender element tests were adopted in line with previous research performed by Shi et al. (2019) using the same laboratory equipment and similar soil materials. Thus, a single-cycle sinusoidal pulse wave was selected as the excitation signal at a frequency of 15 kHz and a voltage with an amplitude of 20 V for the transmitting bender element. Besides, the peak-to-peak method was selected as the interpretation method for shear wave travel time as other time domain and cross-correlation methods were found to be highly affected by near-field effects and reflected P-waves. After the transmitted and received waveforms were captured on the oscilloscope, digitised data was processed for the determination of shear wave propagation time (t) between the bender elements tip-to-tip distance ($L_{t\text{-}t}$), assuming this is the correct travel length for the shear waves, as suggested by Dyvik & Olsen (1989). The effects of selecting the bender elements mid-to-mid distance as the travel length is provided for comparison. The propagation time was defined as the time difference between the positive peak of the transmitted signal trace and the peak of the first significant wave of the receiver signal trace (see Figure 4). Hence, the shear wave velocity V_s (m/s) for each bender element test was calculated according to Eq. 1:

$$V_s = L_{t-t}/t \tag{1}$$

And then, the small-strain shear modulus G_{max} (MPa) of the sand specimen is estimated based on the elastic wave propagation theory for a homogeneous medium (see Eq. 2):

$$G_{max} = \rho {V_s}^2 \tag{2}$$

where ρ corresponds to the total mass density of the specimen.

3 TEST RESULTS

Figure 4 presents the typical waveforms traces recorded by the digital oscilloscope coming from the transmitted and received electrical signals for all bender element tests performed in this experimental investigation. The figure displays the shear wave departure and arrival times visually identified and used to compute the shear wave propagation time.

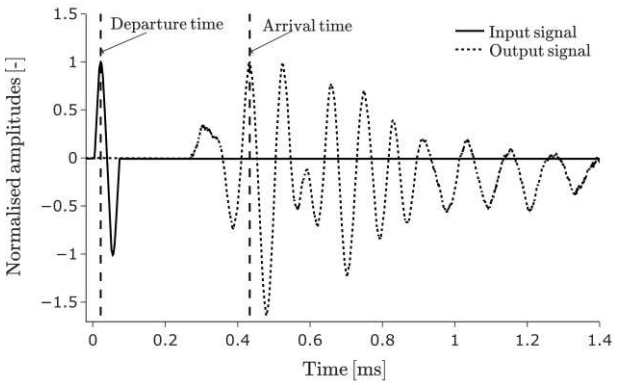

Figure 4. Typical waveform traces recorded by the oscilloscope.

Aiming to verify the degree of repeatability offered by the bender element test setup, G_{max} was measured in different specimens with the same sand material at similar relative density conditions and equal consolidation stress level (TE-02, TE-03 and TE-04). The maximum G_{max} difference for Eemian sand specimens with medium-dense relative density conditions was between 1.3% and 2.4%, which was deemed sufficiently low for successful repeatability conditions. Table 3 provides the bender element test results for Eemian sand specimens at the corresponding effective consolidation stress conditions.

Eemian sand specimen TE-01 had to be tested in partially saturated conditions due to technical issues with the sample back-pressure line. There was an increase in the small-strain shear modulus for this specimen of 10.5% compared with the average value for medium-dense saturated specimens at a consolidation stress level of 85 kPa. This rise in maximum stiffness was the result of a denser specimen and the expected increase in effective stresses, and thus rigidity of the soil skeleton, due to the matric suction induced within the soil matrix.

The effect of a preconsolidation stage on G_{max} measurement for sands was investigated for Eemian specimen TE-02. An effective preconsoldation stress of 251 kPa was applied to this specimen yielding an OCR of 1.48 and 2.95 for the corresponding consolidation pressure. Testing results show a negligible effect of a preconsolidation stage on the estimation of

the small-strain shear modulus of Eemian sand with a maximum G_{max} increment of 1.3%. However, as the OCR values for these tests were relatively low, for higher ratios this conclusion may not apply.

Table 3. Bender element testing results for Eemian sand specimens.

Specimen ID	σ'_c (kPa)	V_s (m/s)	G_{max} (MPa)
TE-01	85	225.7	91.9
	150	257.4	119.6
TE-02	85	204.5	82.5
	170	249.6	122.9
TE-03	85	205.3	82.6
	170	248.8	121.3
TE-04	85	206.3	84.5
	105	218.0	94.4
	170	248.0	122.1

The bender element test results for each Wemmel sand specimen at the corresponding effective consolidation stress conditions are presented in Table 4. These results show a slight increment between 9.5% to 10.8% of the maximum stiffness G_{max} for the two Wemmel specimens when increasing the relative density from dense (D_r = 71%) to very dense (D_r = 87%) conditions.

Regarding the effect of assuming the shear wave travel length as the bender elements mid-to-mid distance, it was found an average increase in shear wave velocity of 6.5% which would result in a 13.5% average increase in G_{max}.

Table 4. Bender element testing results for Wemmel sand specimens.

Specimen ID	σ'_c (kPa)	V_s (m/s)	G_{max} (MPa)
TW-01	135	182.5	63.0
	315	229.4	99.6
TW-02	135	190.5	69.9
	315	238.1	109.1

4 BENCHMARKING WITH IN-SITU TEST MEASUREMENTS AND CPT CORRELATIONS

In-situ testing is an integral part of geotechnical characterization of the stress-strain and strength behaviour for large volumes of ground materials at any OWT farm development. Current bender element testing results were benchmarked with in-situ testing measurements carried out with the seismic piezocone technique (S-PCTP) and correlations with piezocone (PCPT) results obtained on the same geological soil units from the Belgian North sea.

As noted by several authors (e.g. Carlton & Pestana 2016, Menq 2003, Mayne & Rix 1996), measurements of the shear wave velocity (and estimation of G_{max}) for soil materials is best achieved or more accurate at in-situ conditions by means of geophysical methods such as the seismic piezocone technique. This is the case as the soil is investigated through full-scale testing under site-specific anisotropic stress levels, with negligible sample disturbance effects from the testing technique and without losing its fabric or potential cementation. However, field seismic testing is not economically feasible at every OWT location, and therefore, it is common practice to employ different empirical relationships or correlations between G_{max} (or V_s) and cone tip resistance (q_c) for small-strain stiffness estimation (e.g. Rix & Stokoe 1991, Robertson & Cabal, 2015). Therefore, it is valuable to compare the test results obtained in the laboratory with those from other methods or correlations in order to control or evaluate the accuracy of the final measurements.

The S-PCPT technique was performed employing a dual array of geophones incorporated in the cone penetrometer at a fixed vertical spacing. This geophones setup allowed the measurement of shear wave velocity at discrete soil profile depths by cross-correlation of the signals from each individual geophone.

Two main correlations were used to estimate small-strain shear modulus for both types of sands tested in the current laboratory programme. The first correlation was proposed by Rix & Stokoe (1991) for uncemented cohesionless quartz materials based on the cone tip resistance and vertical effective stress according to Eq. 3 for the average value of the correlation range:

$$G_{max} = 1634(q_c)^{0.25}(\sigma'_{vo})^{0.375} \quad (3)$$

where G_{max}, q_c and σ'_{vo} are in kPa. This empirical relationship was developed by adjusting the correlation proposed by Baldi et al. (1989) based on additional laboratory (resonant column and calibration chamber testing) and in-situ (cross-hole and CPT testing) calibration test measurements of G_{max} and q_c. It is important to note that this correlation has an uncertainty band of ±50% on the modulus estimate.

Another well-known relationship employed for comparison was proposed by Robertson & Cabal (2015) for uncemented Quaternary soil deposits, in which shear wave velocity is correlated with the soil behaviour type index (I_c) and net cone resistance (q_n) according to Eq. 4:

$$V_s = [\alpha_{vs}(q_t - \sigma_{vo})/P_a]^{0.5}; where\ \alpha_{vs} = 10^{(0.55I_c+1.68)} \quad (4)$$

where shear wave velocity (V_s) is in m/s and total cone resistance (q_t), in-situ total vertical stress (σ_{vo}) and atmospheric pressure (P_a) are in kPa. G_{max} is then estimated according to equation (2). This correlation is based on S-CPT data and applies to both, cohesive and cohesionless soil materials.

Figure 5 depicts a comparison of the measured and correlated small-strain shear modulus values for the Eemian sand material. S-PCPT measurements were only available for this soil unit. When comparing BE with S-PCPT measurements, it is observed that BE test results considerably underestimated field G_{max} values from 31% to 47%, neglecting the outliers around 50 MPa. This discrepancy agrees with the general consensus that laboratory-based measurements of G_{max} are consistently lower than field seismic techniques due to sample disturbance and other factors mentioned earlier, in addition to the duration of the confining pressure which may induce higher modulus due to a long-term time effect as concluded by Anderson & Stokoe (1978). Regarding the empirical correlations, both relationships overpredicted laboratory G_{max} values by 40% and 99%, respectively, for soil profile depths above 10.0 meters. Below 10.0 meters deep, the average estimate from the Rix & Stokoe (1991) correlation is in good agreement with the BE measurements, while Robertson & Cabal (2015) predictions have a significantly larger range and the BE results lie below the average of this G_{max} range. These discrepancies between laboratory and cone correlations for G_{max} values are congruent with the findings of Chiara & Stokoe (2006), which proposed a quantitative relationship to predict the field V_s based on laboratory measurements and found that laboratory G_{max} values may underestimate the actual field G_{max} value by 40% on average for soil specimens with a laboratory-based shear wave velocity of around 200 m/s. This is equivalent to an increment of field G_{max} values from 60% to 70% of the values obtained in the laboratory, disregarding long-term confining time effects.

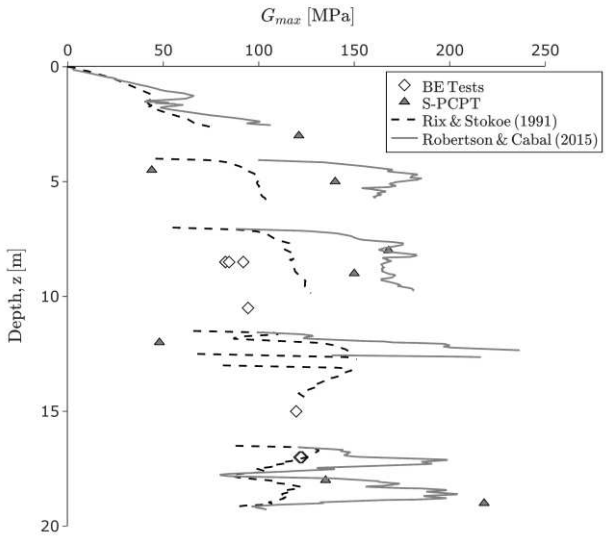

Figure 5. Bender element G_{max} measurements compared with in-situ testing and correlations.

Figure 6 plots the bender element testing and PCPT correlations results for the Wemmel soil unit. The BE results were separated between dense and very dense conditions and the results of the correlations came from two PCPT boreholes with a different stratigraphic location of the Wemmel sand layer. To estimate G_{max} according to the relationship proposed by Robertson & Cabal (2015) it was necessary to calculate the normalised cone parameters assuming a hydrostatic pore water pressure scenario, as a small 5 cm^2 cone without pore pressure sensor was employed and then u_2 measurements were not available for the Wemmel sand layer. The figure shows a low increment in G_{max} for BE sand specimens with an increase of relative density from 71% to 87%. A higher stiffness modulus rise was found for deeper sand layers, highlighting the dependence on the effective geostatic state of stresses for soil shear modulus at small-strains. On a similar trend as for the Eemian sand results, the correlations by Rix & Stokoe (1991) and Robertson & Cabal (2015) estimated G_{max} values significantly higher compared to the BE test results for the Wemmel sand, with increments in between 80% to 459% for the average values of the correlations, respectively. To a certain extent, this high difference between correlations increments may be explained by the fact that the estimates by Rix & Stokoe (1991) are average values that can fluctuate in a range of ±50%, which in case of a higher boundary value, would yield a closer G_{max} estimate between both correlations. Additionally, very dense relative density conditions in the Wemmel sand layer generated early and continuous cone penetration refusals, which led to a very wide range of G_{max} values estimated by the used correlations, especially by Robertson & Cabal (2015) due to a higher exponent value for the cone resistance parameter in the formulation. When comparing G_{max} data from BE testing and piezocone correlations, it is evident that the laboratory results match with a lower bound of the empirical correlations. This fact supports the previous testing results regarding important discrepancies between laboratory testing and empirical correlations or in-situ testing for small-strain shear modulus, which are attributed mainly due to soil disturbance and testing scale effects, as the scale of the measurement also plays a key role in the determination of shear wave velocity in the soil.

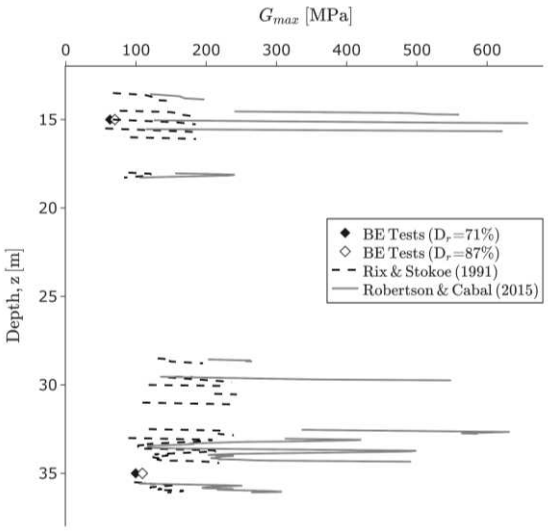

Figure 6. Bender element G_{max} measurements compared with CPT correlations.

5 CONCLUSIONS

This paper describes the execution and analysis of an experimental investigation to assess the small-strain shear modulus G_{max} of Belgian North Sea soils in the laboratory through a bender element setup on a stress path triaxial cell. The measurements were compared with seismic piezocone testing results and with empirical piezocone correlations commonly employed in the offshore geotechnical industry.

Effective repeatability conditions for the bender element test setup were proven with a maximum G_{max} result difference of 2.4% for independent tests results with equivalent testing conditions. The bender element testing results consistently reported G_{max} values close or at the lower boundary of the range of values predicted by in-situ measurements and piezocone correlations. These results are consistent with the findings of previous research that attribute the relatively low values of laboratory-based G_{max} measurements to sample disturbance, testing scale effects and long-term confining time effects. It is important to emphasise the need of correlating advanced laboratory testing, seismic field measurements and empirical relations aiming to accurately characterise the soil maximum shear modulus, as an integrated use of these tools is effective in reducing the uncertainty in the determination of soil parameters to be used in dynamic deformation analysis.

This experimental research provides a new benchmark for maximum stiffness measurements of soil materials in the region, which can assist in the prediction of the dynamic performance of offshore wind turbines monopiles aiming to optimize the design of future wind farms developments.

Further work is ongoing to evaluate cyclic soil element tests to advance understanding of the complex behaviour of OWT monopiles by replicating offshore loading conditions and calibrating numerical pile response models. Advanced laboratory testing is essential to progress on the modelling of the detailed cyclic constitutive behaviour of the ground.

6 ACKNOWLEDGEMENTS

The research presented herein was performed in the context of the SOILTWIN project with the financial support of VLAIO (Flander Innovation Agency). Technicians F.V. Boxstael and J. Van der Perre are thanked also for their support in the laboratory. The use of Groundhog Python package for automated

geotechnical calculations and plotting is acknowledged and recommended.

7 REFERENCES

Aasen S., Page A.M., Skau K.S. and Nygaard T.A. 2017. Effect of foundation modelling on the fatigue lifetime of a monopile-based offshore wind turbine. *Wind Energ. Sci.*, 2, 361–376.

Anderson D.G. and Stokoe K.H. 1978. Shear Modulus: A Time-Dependent Soil Property. *Dynamic Geotechnical Testing*. ASTM STP 654, ASTM, 66 – 90.

ASTM. 2006. Standard test methods for maximum index density and unit weight of soils using a vibratory table. ASTM standard D4253. *ASTM International*, West Conshohocken, Pa.

Baldi G., Bellotti R., Ghionna V., Jamiolkowski M. and Lo Presti D.C.F. 1989. Modulus of sands from CPTs and DMTs. *Proc. XII ICSMFE*, Rio de Janeiro.

Byrne B.W., McAdam R.A., Burd H.J., Houlsby G.T., Martin C.M., Beuckelaers W.J.A.P., Zdravkovic L. et al. 2017. PISA: New Design Methods for Offshore Wind Turbine Monopiles. *Proc. OSIG 2017*, London.

Carlton B.D. and Pestana J.M. 2019. A unified model for estimating the in-situ small strain shear modulus of clays, silts, sands and graves. *Soil Dyn. Earthq. Eng.* 88, 345-355.

Chiara N. and Stokoe K.H. 2006. Sample disturbance in resonant column test measurement of small strain shear wave velocity. *Proc. Soil Stress-Strain Behavior: Measurement, Modeling and Analysis*, 605-613.

Dyvik R. and Olsen T.S. 1989. G_{max} measured in oedometer and DSS tests using bender elements. *Proc. XII ICSMFE,* Rio de Janiero. 39-42.

Jardine R.J. 2014. Advanced laboratory testing in research and practice: the 2nd Bishop lecture. *Geotechnical Research*. 1, 2-31.

Knudsen S., Lunne T., V.S. Quinteros, Vestgarden T., Krogh L. and Pedersen R.D. 2019. Effect of reconstitution techniques on the triaxial stress-strength behaviour of a very dense sand. *Proc. XVII ECSMGE.*

Menq F-Y. 2003. Dynamic Properties of Sandy and Gravelly Soils. *PhD dissertation, Univ. of Texas at Austin*, Austin, Texas.

Rix G.L. and Stokoe K.H. 1991. Correlation of initial tangent modulus and cone penetration resistance. *Proc. 1st Int. Sym. Calibration Chamber Testing*. 351-362.

Robertson P.K. and Cabal K.L. 2015. Guide to Cone Penetration Testing for Geotechnical Engineering. *Signal Hill, California: Gregg Drilling & Testing, Inc.*

Shi J., Haegeman W. and Cnudde V. 2019. Anisotropic small-strain stiffness of calcareous sand affected by sample preparation, particle characteristics and gradation. *Géotechnique*. 71(4), 305-19.